IEEE Access
Multidisciplinary | Rapid Review | Open Access Journal

SPECIAL SECTION ON ADVANCED CONTROL AND HEALTH MANAGEMENT FOR AIRCRAFT AND ITS PROPULSION SYSTEM

Received July 6, 2017, accepted July 18, 2017, date of publication July 24, 2017, date of current version August 22, 2017.

Digital Object Identifier 10.1109/ACCESS.2017.2731425

A Fault-Tolerant Cooperative Positioning Approach for Multiple UAVs

YAOHONG QU[1], JIZHI WU[2], BING XIAO[3], (Member, IEEE), AND DONGLI YUAN[1]

[1]School of Automation, Northwestern Polytechnical University, Xi'an 710072, China
[2]Department of Flight Control System, Commercial Aircraft Corporation of China Ltd., Shanghai 200126, China
[3]College of Engineering, Bohai University, Jinzhou 121013, China

Corresponding author: Bing Xiao (bxiaobing@gmail.com)

This work was supported in part by the National Natural Science Foundation of China under Grant 61473229 and Grant 61503035 and in part by the China Postdoctoral Science Foundation founded project under Grant 2016M590456 and Grant 2017T100369.

ABSTRACT Due to the increasing potentials and benefits of unmanned aerial vehicles (UAVs) in civil and surveillance applications, the cooperative flight using multiple UAVs has attracted more and more attention. However, fault-tolerant cooperative positioning for malfunctions in global positioning system (GPS) is one of the challenges that need to be addressed in various practical applications of UAVs. Motivated by solving this issue, this paper presents a reliable cooperative positioning approach for multiple UAVs cooperative flight by using the geometric azimuth angle and the inclination angle relative to the reference UAVs. In this proposed cooperative positioning system (COPS), these relative angles are measured through radio direction finding equipped on UAVs. With the horizontal dilution of precision of the various reference UAVs carefully analyzed, the optimal reference UAVs set can be first selected. Based on a constant acceleration kinematic model, an extended Kalman filter is then employed to improve the positioning accuracy. A COPS/GPS fault-tolerant navigation algorithm is finally developed to accommodate GPS fault. Simulation results are further presented to verify that the proposed algorithm can guarantee satisfactory navigation of the UAVs even when their GPS cannot work.

INDEX TERMS Unmanned aerial vehicle, cooperative positioning system, extended Kalman filter, horizontal dilution of precision.

I. INTRODUCTION

Cooperative flight using multiple UAVs is becoming a research hot due to the increasing demands of using multiple smaller and lower-cost UAVs to replace single, larger, and higher-cost UAV. Examples include spacecraft formation flying [1], [2], UAV formation flying [3], [4], coordinated rendezvous of UAVs [5], and coordinated path planning [6]. It should be noted that almost all the existing results are proposed based on a strict assumption, *i.e.*, the navigation systems of UAVs operate normally. However, this assumption would be not satisfied in practical applications. As such, cooperative flight of multiple UAVs in case of faulty navigation subsystem should be addressed [7]–[9], and it is still an open problem.

It is well-known that reliability should be ensured for any safety-critical systems such as aircrafts and UAVs. In accordance with this, fault-tolerant capability is also required for the UAV navigation systems. This is known as fault-tolerant navigation systems (FTNS). It is similar as the role of fault-tolerant control systems (FTCS) [10]–[14]. From the standpoint of FTCS, FTNS are still a new topic. There are few investigations for multiple UAVs of cooperative or formation flight. Currently, there are only several results on fault-tolerant navigation and localization methods for single UAV by integrating INS (inertial navigation system) with GPS [15], [16]. However, this kind of INS/GPS integrated fault-tolerant navigation system cannot satisfy the demand of long-time cooperative flight when GPS is faulty. To avoid such drawback, more and more attention has been paid to cooperative positioning to improve fault-tolerance of navigation by using relative range and/or relative angle information between UAVs to calculate the position, as suggested in [1], [2] and [19]. That is because the relative range measurements can be obtained using either ultra-wideband (UWB) radio technology or optical systems [20], [21]. Moreover, with the development of the radio direction finding (RDF) techniques [23]–[25], the relative angles between UAVs

could be measured and utilized to achieve precise cooperative positioning.

This paper focuses on solving the multiple UAVs cooperative positioning problem in the presence of GPS transient failures by using the relative azimuth angle and the relative inclination angle. The main contributions of the study can be summarized as:

1) The geometric positioning model of the faulty UAV utilizing the relative location to the two reference UAVs, which are selected based on the minimum HDOP principle, is presented.

2) A constant acceleration kinematic model is established and an extended Kalman filter (EKF) is employed to improve the positioning accuracy based on the proposed model.

3) A COPS/GPS fault-tolerant navigation algorithm is developed using a Chi-squared residual testing scheme to accommodate the GPS faults.

The paper is organized as follows: In Section II, the problem to be investigated is formulated. Section III introduces the geometric model of the cooperative positioning system. Section IV describes the COPS/GPS fault-tolerant navigation algorithm of UAVs. Simulation results of applying the proposed algorithm to a multiple UAVs cooperative positioning are shown in Section V to verify the effectiveness of the approach. The paper is ended with conclusions given in Section VI.

II. PROBLEM FORMULATION

It is assumed that each UAV is equipped with GPS receiver. The position information of any UAV is shared with each other through wireless communication. Each UAV is equipped with a set of transmitter and receiver of radio direction finding (RDF) to measure the azimuth angle and the inclination angle between each two UAVs. In general, the radio signal is emitted from the RDF transmitter on the faulty UAV and received by the RDF receiver on healthy UAV. The relative angles are decoded by the healthy UAVs and transmitted back to the faulty UAV along with their own current positions. Then, the position of faulty UAV can be calculated according to cooperative positioning model utilizing the relative angle information and the position information of reference UAVs.

In this paper, the number of reference UAVs is assumed to be larger than two. This is the minimum reference UAVs required for cooperative positioning. Accordingly, the reference UAVs can be divided into several reference sets. It means that the cooperative positioning has certain level of information redundancy. Hence, it is necessary to find out the optimal reference UAVs set based on the minimal horizontal dilution of precision (HDOP) to calculate the position of the faulty UAV. To further improve the accuracy of the cooperative positioning, an extended Kalman filter is then employed in each UAV based on a constant acceleration kinematic model. A COPS/GPS fault-tolerant navigation algorithm based on a Chi-squared residual test against GPS fault is finally developed.

III. COOPERATIVE POSITIONING SYSTEM

Each UAV is equipped with a radio direction finder which consists of radio transmitter and receiver. The azimuth angle and the inclination angle among each two UAVs can be measured through radio direction finder. As a result, the relative position of the faulty UAV relative to the reference UAVs can be obtained through geometric interpretation. Then, the absolute location can be calculated by adding the position of reference UAV. Especially, the radio direction finder can measure the relative azimuth angle and the inclination angle regularly under the condition that the range between RDF transmitter and receiver is less than the operating range threshold. This threshold is usually tens of kilometers.

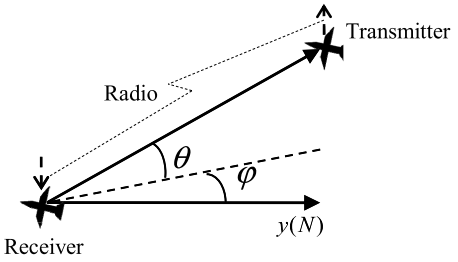

FIGURE 1. The relative geometric angle relationship of two terminals.

In the coordinate frame with the x-axis pointing to the east direction, the y-axis pointing to the north direction, the z-axis determined according to right-hand rule, and the origin selected arbitrarily on the earth, the azimuth angle is defined as the angle of projection of radio transmitting direction in horizontal plane relative to north direction and denoted by φ. The inclination angle is defined as the angle of radio transmitting direction relative to horizontal plane and denoted by θ. Figure 1 shows a typical single-directional transmitting radio signal between any two UAVs. The wireless radio signal is transmitted through the antenna of RDF on the ''Transmitter'' UAV. The ''Receiver'' UAV would receive the radio signal which is utilized to recognize the azimuth and inclination angles through RDF. The current position information of the ''Transmitter'' UAV is packed in the radio signal and obtained by the ''Receiver'' UAV.

To obtain the position of a faulty UAV, it necessitates two sets of azimuth angle and inclination angle at least. In this work, the cooperative positioning utilizing two reference UAVs is discussed. Because the number of all the reference UAVs is more than two, there exists one optimal reference UAVs set with minimum error propagation statistically, when considering the different spatial geometric distribution of reference UAVs. In other words, the cooperative positioning system can find out the optimal reference UAVs set from multiple reference UAVs through analyzing the relative azimuth angle, the inclination angle, and the position of reference UAVs.

A. MODELING OF THE COOPERATIVE POSITIONING SYSTEM

Suppose that the multiple UAVs are flying in the airspace where all the UAVs can communicate with each other. Each UAV can measure the relative angles to the others. Among these UAVs, GPS of one UAV becomes unreliable (now, such UAV is denoted as faulty UAV). However, RDF of this faulty UAV can continue to transmit a radio signal. The other UAVs can receive the radio signal and send the measured relative azimuth angle and inclination angle along with their current positions back. Figure 2 illustrates a simplified distribution of multiple UAVs with the faulty UAV denoted by U^f and the reference UAVs denoted by U_i^r $(i = 1, 2, \ldots, n)$. The faulty UAV has a relative geometric relationship with each reference UAVs, as we can see in Fig. 1. All the reference UAVs can position themselves through GPS using received signals from satellites and can share their positions with the faulty UAV.

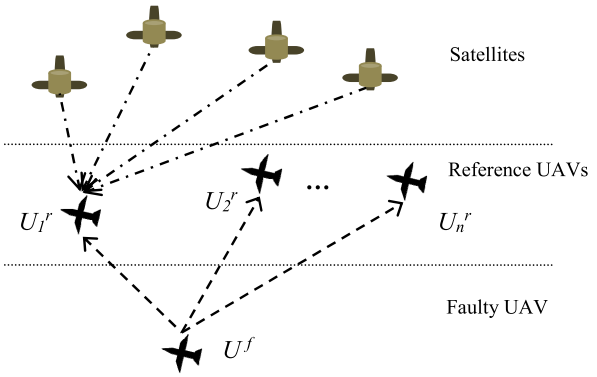

FIGURE 2. Hierarchy chart of absolute positioning and relative positioning.

Let the positions of the reference UAVs and the faulty UAV be denoted as $\boldsymbol{X}_i = (x_i\ y_i\ z_i)^{\mathrm{T}}$, $i = 1, 2, \ldots, n$, and $\boldsymbol{X} = (x\ y\ z)^{\mathrm{T}}$, respectively. The relative inclination angle and the azimuth angle are denoted by θ_i and φ_i, respecitvely, where subscript $i$indicates the relative relationship between faulty UAV and reference UAV U_i^r. The range vector from reference UAV to faulty UAV is denoted by $\boldsymbol{r}_i = (x_i^r\ y_i^r\ z_i^r)^{\mathrm{T}}$. Taking U_1^r and U_2^r as the reference UAVs for convenience of modeling in the following sections, two corresponding sets of inclination angles and azimuth angles are $(\theta_1\ \varphi_1)$ and $(\theta_2\ \varphi_2)$. Because these angles cannot directly derive the position of faulty UAV, the range vector $\boldsymbol{r}_1$ and $\boldsymbol{r}_2$ are calculated as:

$$\boldsymbol{r}_1 = \boldsymbol{X} - \boldsymbol{X}_1 = (x - x_1 \quad y - y_1 \quad z - z_1)^{\mathrm{T}} \tag{1}$$

$$\boldsymbol{r}_2 = \boldsymbol{X} - \boldsymbol{X}_2 = (x - x_2 \quad y - y_2 \quad z - z_2)^{\mathrm{T}} \tag{2}$$

where $(x_1^r\ y_1^r\ z_1^r)$ and $(x_2^r\ y_2^r\ z_2^r)$ represent the relative tri-axis variations of two reference UAVs' positions in the inertial coordinate frame, respectively. By using the measured azimuth angle and inclination angle, these three relative variations can also be explicitly obtained as:

$$\boldsymbol{r}_i = ||\boldsymbol{r}_i|| \begin{pmatrix} \cos\theta_i \sin\varphi_i \\ \cos\theta_i \cos\varphi_i \\ \sin\theta_i \end{pmatrix}, \quad i = 1, 2 \tag{3}$$

where

$$||\boldsymbol{r}_i|| = \sqrt{(x_i^r)^2 + (y_i^r)^2 + (z_i^r)^2}, \quad i = 1, 2 \tag{4}$$

Although the relative distance $||\boldsymbol{r}_i||$ between the faulty and the reference UAV i is unknown, the relative location between two reference UAVs can be calculated by comparing their positions provided by GPS receiver. The relative range vector $\boldsymbol{r}_{12}$ between U_1^r and U_2^r can be determined as:

$$\boldsymbol{r}_{12} = \boldsymbol{r}_1 - \boldsymbol{r}_2 = \boldsymbol{X}_2 - \boldsymbol{X}_1 \tag{5}$$

According to Eqs. (1)-(4), Eq. (5) can be re-written into the following matrix/vector form:

$$\boldsymbol{r}_{12} = \begin{pmatrix} x_2 - x_1 \\ y_2 - y_1 \\ z_2 - z_1 \end{pmatrix} = \begin{pmatrix} \cos\theta_1 \sin\varphi_1 & -\cos\theta_2 \sin\varphi_2 \\ \cos\theta_1 \cos\varphi_1 & -\cos\theta_2 \cos\varphi_2 \\ \sin\theta_1 & -\sin\theta_2 \end{pmatrix} \times \begin{pmatrix} ||\boldsymbol{r}_1|| \\ ||\boldsymbol{r}_2|| \end{pmatrix} \tag{6}$$

or

$$\boldsymbol{r}_{12} = \boldsymbol{S}_{12}\boldsymbol{\chi} \tag{7}$$

where $\boldsymbol{S}_{12} \in \Re^{3\times 2}$, $\boldsymbol{\chi} \in \Re^2$, and $\boldsymbol{r}_{12} \in \Re^3$. The solution $\boldsymbol{\chi}$ of Eq. (7) can be obtained through least square method. Multiplying $\boldsymbol{S}_{12}^{\mathrm{T}}$ to both sides of Eq. (7) leads to

$$\boldsymbol{S}_{12}^{\mathrm{T}}\boldsymbol{r}_{12} = (\boldsymbol{S}_{12}^{\mathrm{T}}\boldsymbol{S}_{12})\boldsymbol{\chi} \tag{8}$$

The least square solution can be obtained by:

$$\boldsymbol{\chi} = (\,||\boldsymbol{r}_1|| \quad ||\boldsymbol{r}_2||\,)^{\mathrm{T}} = (\boldsymbol{S}_{12}^{\mathrm{T}}\boldsymbol{S}_{12})^{-1}\boldsymbol{S}_{12}^{\mathrm{T}}\boldsymbol{r}_{12} \tag{9}$$

To guarantee the existence of a solution $\boldsymbol{\chi}$, matrix $\boldsymbol{S}_{12}$ should satisfy the following condition:

$$rank(\boldsymbol{S}_{12}^{\mathrm{T}}\boldsymbol{S}_{12}) = rank(\boldsymbol{S}_{12}) = 2 \tag{10}$$

The least square solution gives out the two relative ranges between the faulty and the reference UAV. Hence, the position of faulty UAV can be calculated according to

$$\boldsymbol{X} = \boldsymbol{X}_i + \boldsymbol{r}_i = \begin{pmatrix} x_i \\ y_i \\ z_i \end{pmatrix} + ||\boldsymbol{r}_i|| \begin{pmatrix} \cos\theta_i \sin\varphi_i \\ \cos\theta_i \cos\varphi_i \\ \sin\theta_i \end{pmatrix}, \quad i = 1, 2 \tag{11}$$

which implies that the position of the faulty UAV can be calculated by using the position and the relative range of either U_1^r or U_2^r.

B. MODELING OF THE HORIZONTAL COOPERATIVE POSITIONING SYSTEM

Assume that there is one scenario, *i.e.*, all the UAVs are flying in the same constant height. The relative inclination angle between any two UAVs equals to zero. Then, Eq. (3) can be simplified as:

$$\begin{pmatrix} x - x_i \\ y - y_i \end{pmatrix} = ||r_i|| \begin{pmatrix} \sin\varphi_i \\ \cos\varphi_i \end{pmatrix}, \quad i = 1, 2 \tag{12}$$

Then, the range variable $||r_i||$ can be eliminated by introducing the tangent function of azimuth angle

$$x - x_1 = (y - y_1)\tan\varphi_1 \tag{13}$$
$$x - x_2 = (y - y_2)\tan\varphi_2 \tag{14}$$

If the solution of Eq. (13) and Eq. (14) exists, then the position of faulty UAV can be derived as

$$\begin{pmatrix} x \\ y \end{pmatrix} = \begin{pmatrix} 1 & -\tan\varphi_1 \\ 1 & -\tan\varphi_2 \end{pmatrix}^{-1} \begin{pmatrix} x_1 - y_1\tan\varphi_1 \\ x_2 - y_2\tan\varphi_2 \end{pmatrix} \tag{15}$$

Therefore, the following condition should be satisfied to guarantee existence of the solution.

$$\varphi_1 - \varphi_2 \neq k\pi, \quad k = 0, \pm 1 \ldots \tag{16}$$

C. OPTIMAL POSITIONING IN HORIZONTAL PLANE

It is worth mentioning that all the relative angles are measured with noises. Different spatial geometric distributions lead to different error propagation. It is necessary to determine the optimal reference UAVs set based on a horizontal geometric positioning model. Taking the combination of reference UAVs U_1^r and U_2^r as example, the azimuth measurement can be written from Eqs. (13)-(14) into the following nonlinear form:

$$\boldsymbol{\Omega} = \boldsymbol{f}(\boldsymbol{X}) + \boldsymbol{V} \tag{17}$$

where the vector $\boldsymbol{X} = (x\ y)^{\mathrm{T}}$ is the horizontal position coordinate of the faulty UAV to be determined, $\boldsymbol{\Omega} = (\varphi_1\ \varphi_2)^{\mathrm{T}}$ is the relative azimuth angles between the faulty UAV and either of two reference UAVs, $\boldsymbol{f}(\boldsymbol{X}) = (\boldsymbol{f}_1(\boldsymbol{X})\,\boldsymbol{f}_2(\boldsymbol{X}))^{\mathrm{T}}$ indicates the arctangent function, and $\boldsymbol{V} = (v_1\ v_2)^{\mathrm{T}}$ is the Gaussian white noise with zero-mean:

$$\boldsymbol{E}(\boldsymbol{V}\boldsymbol{V}^{\mathrm{T}}) = \begin{pmatrix} \boldsymbol{E}(v_1)^2 & \boldsymbol{E}(v_1v_2) \\ \boldsymbol{E}(v_2v_1) & \boldsymbol{E}(v_2)^2 \end{pmatrix} = \begin{pmatrix} \sigma^2 & 0 \\ 0 & \sigma^2 \end{pmatrix} = \boldsymbol{R} = \sigma^2\boldsymbol{I} \tag{18}$$

In this paper, the optimal position is considered as the one whose radial error tends to be the minimum. To determine optimal positioning, the index of minimum variance estimation is defined as:

$$\begin{aligned} \boldsymbol{J} &= \boldsymbol{E}\{[\boldsymbol{X} - \hat{\boldsymbol{X}}(\boldsymbol{\Omega})]^T[\boldsymbol{X} - \hat{\boldsymbol{X}}(\boldsymbol{\Omega})]\} \\ &= \boldsymbol{E}((\hat{x} - x)^2 + (\hat{y} - y)^2) = \min \end{aligned} \tag{19}$$

where $(x\ y)$ is the position of the faulty UAV, and $(\hat{x}\ \hat{y})$ is the estimated position based on the relative angle measurement.

Because the relationship between the measurement $\boldsymbol{\Omega}$ and the position $\boldsymbol{X}$ is nonlinear, the Taylor series expansion can be introduced:

$$\boldsymbol{f}(\boldsymbol{X}) = \boldsymbol{f}(\hat{\boldsymbol{X}}) + \frac{\partial \boldsymbol{f}(\boldsymbol{X})}{\partial \boldsymbol{X}^T}|_{\boldsymbol{X}=\hat{\boldsymbol{X}}}(\boldsymbol{X} - \hat{\boldsymbol{X}}) + \boldsymbol{H}.\boldsymbol{O}.\boldsymbol{T} \tag{20}$$

where $\boldsymbol{H}.\boldsymbol{O}.\boldsymbol{T}$ stands for "higher-order terms", and it can be omitted. By introducing the following variables:

$$\delta\boldsymbol{X} = \boldsymbol{X} - \hat{\boldsymbol{X}} \tag{21}$$
$$\delta\boldsymbol{\Omega} = \boldsymbol{f}(\boldsymbol{X}) - \boldsymbol{f}(\hat{\boldsymbol{X}}) \tag{22}$$
$$\boldsymbol{F} = \frac{\partial \boldsymbol{f}(\boldsymbol{X})}{\partial \boldsymbol{X}^T}|_{\boldsymbol{X}=\hat{\boldsymbol{X}}} \tag{23}$$

Equation (20) can be written as:

$$\delta\boldsymbol{\Omega} = \boldsymbol{F}\delta\boldsymbol{X} \tag{24}$$

Since the matrix $\boldsymbol{F}$ in Eq. (24) is nonsingular, its solution can be obtained as:

$$\delta\boldsymbol{X} = \boldsymbol{F}^{-1}\delta\boldsymbol{\Omega} \tag{25}$$

where $\boldsymbol{F} \in \Re^{2\times 2}$ is partial differential Jacobian matrix of function $\boldsymbol{f}$,

$$\boldsymbol{F} = \begin{pmatrix} \frac{\partial \boldsymbol{f}_1(\boldsymbol{X})}{\partial x}|_{x=\hat{x}} & \frac{\partial \boldsymbol{f}_1(\boldsymbol{X})}{\partial y}|_{y=\hat{y}} \\ \frac{\partial \boldsymbol{f}_2(\boldsymbol{X})}{\partial x}|_{x=\hat{x}} & \frac{\partial \boldsymbol{f}_2(\boldsymbol{X})}{\partial y}|_{y=\hat{y}} \end{pmatrix} \tag{26}$$

The mean squared error matrix is calculated by:

$$\begin{aligned} \boldsymbol{E}(\delta\boldsymbol{X}(\delta\boldsymbol{X})^{\mathrm{T}}) &= \boldsymbol{E}(\boldsymbol{F}^{-1}\delta\boldsymbol{\Omega}(\delta\boldsymbol{\Omega})^{\mathrm{T}}(\boldsymbol{F}^{-1})^{\mathrm{T}}) \\ &= \boldsymbol{F}^{-1}\boldsymbol{E}(\delta\boldsymbol{\Omega}(\delta\boldsymbol{\Omega})^{\mathrm{T}})(\boldsymbol{F}^{T})^{-1} \\ &= \sigma^2(\boldsymbol{F}^{\mathrm{T}}\boldsymbol{F})^{-1} \end{aligned} \tag{27}$$

The horizontal dilution of precision (HDOP), as the optimal index, is defined as the trace of mean squared error matrix, and it is shown as:

$$HDOP = trace(\sigma^2(\boldsymbol{F}^{\mathrm{T}}\boldsymbol{F})^{-1}) \tag{28}$$

According to the implication of the index as given by Eq. (19) or Eq. (28), the radial error tends to be smaller while the HDOP is calculated to be smaller. Consequently, the position in corresponding to the two reference UAVs with minimum HDOP, would be theoretically chosen as the optimal positioning with smallest error propagation.

D. EXTENDED KALMAN FILTER FOR COPS

The two optimal referenced UAVs can be selected with most minor error propagation according to the minimum HDOP principle. However, the measurement errors and noises still need to be processed for high accuracy navigation. To achieve this objective, an extended Kalman filter is employed to improve the positioning accuracy. Based on dead reckoning equations, a kinematic model can be obtained to predict the future position, velocity, and heading. The state variables at time $k-1$ can be expressed as:

$$\boldsymbol{\chi}_{k-1} = (x_{k-1}\ \ y_{k-1}\ \ v^e_{k-1}\ \ v^n_{k-1}\ \ a_{k-1}\ \ \psi_{k-1}\ \ \omega_{k-1})^{\mathrm{T}} \tag{29}$$

After a short sampling period of T, the states at time k can be calculated according to Newton's laws of motion, and it is given by:

$$\begin{aligned}\dot{\boldsymbol{\chi}}_k &= \begin{pmatrix} x_k \\ y_k \\ v_k^e \\ v_k^n \\ a_k \\ \psi_k \\ \omega_k \end{pmatrix} = \begin{pmatrix} x_{k-1} + Tv_{k-1}^e + 0.5T^2 a_{k-1}\cos\psi_{k-1} \\ y_{k-1} + Tv_{k-1}^n + 0.5T^2 a_{k-1}\sin\psi_{k-1} \\ v_{k-1}^e + Ta_{k-1}\cos\psi_{k-1} \\ v_{k-1}^n + Ta_{k-1}\sin\psi_{k-1} \\ a_{k-1} \\ \psi_{k-1} + T\omega_{k-1} \\ \omega_{k-1} \end{pmatrix} \\ &\quad + \boldsymbol{W}_{k-1} \\ &= g(\boldsymbol{\chi}_{k-1}) + \boldsymbol{W}_{k-1} \end{aligned} \tag{30}$$

where x_k and y_k are the position coordinates in east and north directions, respectively. v_k^e and v_k^n are the velocity in east and north direction, respectively. a_k is the acceleration, ψ_k is the heading of UAV, ω_k is the heading rate, and $\boldsymbol{W}_{k-1}$ is the input noise with variance of $\boldsymbol{Q}_{k-1}$. Note that the acceleration and the heading rate are assumed to be equal during the sampling period of T. Since the extended Kalman filter requires the state transition matrix to calculate variance propagation, the transition matrix can be derived as Jacobian matrix of kinematic model as:

$$\begin{aligned}&\boldsymbol{\Phi}_{k-1} \\ &= \begin{pmatrix} 1 & 0 & T & 0 & 0.5T^2\cos\psi_{k-1} & -0.5T^2 a_{k-1}\sin\psi_{k-1} & 0 \\ 0 & 1 & 0 & T & 0.5T^2\sin\psi_{k-1} & 0.5T^2 a_{k-1}\cos\psi_{k-1} & 0 \\ 0 & 0 & 1 & 0 & T\cos\psi_{k-1} & -Ta_{k-1}\sin\psi_{k-1} & 0 \\ 0 & 0 & 0 & 1 & T\sin\psi_{k-1} & Ta_{k-1}\cos\psi_{k-1} & 0 \\ 0 & 0 & 0 & 0 & 1 & 0 & 0 \\ 0 & 0 & 0 & 0 & 0 & 1 & T \\ 0 & 0 & 0 & 0 & 0 & 0 & 1 \end{pmatrix} \end{aligned} \tag{31}$$

The predicted state and the variance propagation of the kinematic model is updated according to

$$\hat{\boldsymbol{\chi}}_{k/k-1} = g(\hat{\boldsymbol{\chi}}_{k-1}) \tag{32}$$

$$\boldsymbol{P}_{k/k-1} = \boldsymbol{\Phi}_{k-1}\boldsymbol{P}_{k-1}\boldsymbol{\Phi}_{k-1}^T + \boldsymbol{Q}_{k-1} \tag{33}$$

where $\boldsymbol{P}_{k-1}$ is the mean-squared variance matrix of state estimation. To obtain more accurate state estimation, new measurements at each sampling period are employed to correct the predicted state of kinematic model. The measurements include the relative angles, velocity, and heading. According to the geometric model of cooperative positioning, the relationship between the relative angle and the position of the faulty UAV is nonlinear. Hence, the observation equation can be expressed by:

$$\zeta_k = \begin{pmatrix} \varphi_k^1 \\ \varphi_k^2 \\ v_k \\ \psi_k \end{pmatrix} = h(\boldsymbol{\chi}_k) + \boldsymbol{V}_k = \begin{pmatrix} \arctan\dfrac{x_k^1 - x_k}{y_k^1 - y_k} \\ \arctan\dfrac{x_k^2 - x_k}{y_k^2 - y_k} \\ v_k \\ \psi_k \end{pmatrix} + \boldsymbol{V}_k \tag{34}$$

where $(x_k^1\ y_k^1)$ and $(x_k^2\ y_k^2)$ represent the positions of two reference UAVs, respectively. $\boldsymbol{V}_k \in \Re^4$ represents the measurements noise with zero-mean and variance of $\boldsymbol{R}_k \in \Re^4$. The relative angles φ_k^1 and φ_k^1 are measured by RDF. The velocity v_k is measured by pitot (The atmosphere wind is ideally considered as still in this paper). The heading angle ψ_k is measured by using magnetic compass (MC) and inertial measurement unit (IMU). Through correction of residual of measurement errors, the state estimation can be obtained as

$$\hat{\boldsymbol{\chi}}_k = \hat{\boldsymbol{\chi}}_{k/k-1} + \boldsymbol{K}_k(\zeta_k - h(\hat{\boldsymbol{\chi}}_{k/k-1})) \tag{35}$$

where the matrix $\boldsymbol{K}_k$ is the weight of observation residual. It contains variance propagation of the kinematic model and variance of measurement errors. Based on the weight matrix, the variance matrix can be derived as:

$$\boldsymbol{K}_k = \boldsymbol{P}_{k/k-1}\boldsymbol{H}_k^{\mathrm{T}}(\boldsymbol{H}_k\boldsymbol{P}_{k/k-1}\boldsymbol{H}_k^{\mathrm{T}} + \boldsymbol{R}_k)^{-1} \tag{36}$$

$$\boldsymbol{P}_k = (\boldsymbol{I} - \boldsymbol{K}_k\boldsymbol{H}_k)\boldsymbol{P}_{k/k-1} \tag{37}$$

where

$$\boldsymbol{H}_k = \begin{pmatrix} \dfrac{\partial h_1}{\partial x_k} & \dfrac{\partial h_1}{\partial y_k} & 0 & 0 & 0 & 0 & 0 \\ \dfrac{\partial h_2}{\partial x_k} & \dfrac{\partial h_2}{\partial y_k} & 0 & 0 & 0 & 0 & 0 \\ 0 & 0 & 0 & 0 & 1 & 0 & 0 \\ 0 & 0 & 0 & 0 & 0 & 0 & 1 \end{pmatrix} \tag{38}$$

To this end, the extended Kalman filter can be achieved through combining Eqs. (32)-(33) and Eqs. (35)-(37).

IV. DEVELOPMENT OF COPS/GPS FAULT-TOLERANT NAVIGATION ALGORITHM

During a cooperative flight mission, the UAVs are all equipped with a set of GPS and COPS. Generally, a UAV is navigated through GPS whose accuracy can be improved through employing extended Kalman filter. The COPS can be viewed as a backup navigation system when GPS is extremely unreliable. Now, COPS would replace GPS to obtain position information. In addition, the outputs of GPS and COPS are combined in one master filter to get more reliable position information. A fault-tolerant navigation algorithm is proposed through combining GPS and COPS, as shown in Fig. 3.

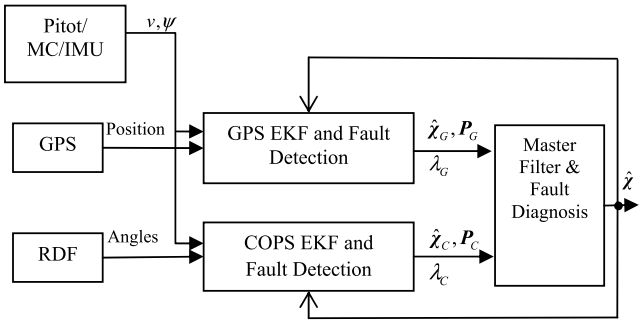

FIGURE 3. Block diagram of COPS-aided fault-tolerant navigation algorithm.

This algorithm involves two integrated sub-filters for GPS and COPS individually with an EKF, both of which can provide fault information. The states estimation and fault states of two sub-filters are then integrated in the master filter to diagnose fault and obtain integrated state estimation $\hat{\chi}$.

A. EXTENDED KALMAN FILTER FOR GPS

The EKF is employed to improve GPS positioning accuracy and detect any potential GPS fault. The kinematic model to be utilized is Eq. (32). Since GPS directly provides position measurements which are different from RDF, the observation equations of GPS should be separately discussed. The observation variables include the position information given by GPS, the velocity, and the heading measurements. It is written by

$$\boldsymbol{Z}_k^g = (\, x_k^g \quad y_k^g \quad v_k \quad \psi_k \,) \tag{39}$$

Then, the observation equation can be written as:

$$\boldsymbol{Z}_k^g = h^g(\boldsymbol{\chi}_k) + \boldsymbol{V}_k^g = \boldsymbol{H}_k^g \boldsymbol{\chi}_k + \boldsymbol{V}_k^g \tag{40}$$

where $\boldsymbol{V}_k^g$ is Gaussian white noise with zero-mean and variance $\boldsymbol{R}_k^g$, and the observation matrix is given by:

$$\boldsymbol{H}_k^g = \begin{pmatrix} 1 & 0 & 0 & 0 & 0 & 0 & 0 \\ 0 & 1 & 0 & 0 & 0 & 0 & 0 \\ 0 & 0 & 0 & 0 & 1 & 0 & 0 \\ 0 & 0 & 0 & 0 & 0 & 0 & 1 \end{pmatrix} \tag{41}$$

With the given observation equation and matrix substituted in five filter equations in Section III.D, the EKF can be implemented for GPS.

B. FAULT DETECTION USING RESIDUAL CHI-SQUARED TEST

In this paper, the COPS is assumed to be always reliable. GPS fault can be detected through assessing the residual of EKF. This residual is defined as the difference between the predicted state and the measurements, and it is given by:

$$\boldsymbol{\gamma}_k = \boldsymbol{Z}_k - \boldsymbol{h}(\hat{\chi}_{k/k-1}) \tag{42}$$

The state estimation $\hat{\boldsymbol{\chi}}_{k/k-1}$ is obtained as position $(\boldsymbol{x}_{k/k-1}\ y_{k/k-1})$ according to Eq. (32) and always corrected by EKF to restrain the accumulative error from the input noise of kinematic model Eq. (30) with zero-mean. Therefore, the residual is mainly determined by the abnormal error contained in observation $\boldsymbol{Z}_k$.

When no fault occurs, the residual is small and close to zero. In case of a fault, the residual becomes larger and changes to non-zero-mean. The variance of the residual can be defined as:

$$\Delta_k = \mathrm{var}(\gamma_k) = \boldsymbol{H}_k \boldsymbol{P}_{k/k-1} \boldsymbol{H}_k^{\mathrm{T}} + \boldsymbol{R}_k \tag{43}$$

where $\boldsymbol{P}_{k/k-1}, \boldsymbol{R}_k$ are the covariance matrix of the state vector error and measurement noise, respectively. The test statistics can be defined as:

$$\lambda_k = \gamma_k^{\mathrm{T}} \Delta_k^{-1} \gamma_k \tag{44}$$

where λ_k is a Chi-squared distribution with a degree of '2'. The fault diagnosis rule is designed as:

$$\begin{cases} \lambda_k > \chi^2_{m,\alpha}, & \textit{Fault} \\ \lambda_k \le \chi^2_{m,\alpha}, & \textit{No fault} \end{cases} \tag{45}$$

The constant threshold $\chi^2_{m,\alpha}$ is determined according to the Chi-square table which is based on confidence level of $(1-\alpha)$. Here, α is the probability of a false alarm.

The variance of the residual contains the variance of both the predicted state and the measurements. When no fault occurs, the variance of measurements is constant. According to Eq. (33), the variance of predicted state consists of the transfer of variance of state estimation in previous step and variance of process noise. However, the time-varying variance of state estimation is far less than $\boldsymbol{Q}_k$, thus can be ignored in Δ_k. Accordingly, one can re-write (34) as:

$$\Delta_k = \boldsymbol{H}_k \boldsymbol{P}_{k/k-1} \boldsymbol{H}_k^{\mathrm{T}} + \boldsymbol{R}_k = \boldsymbol{H}_k \boldsymbol{Q}_k \boldsymbol{H}_k^{\mathrm{T}} + \boldsymbol{R}_k \tag{46}$$

where $\boldsymbol{H}_k$, $\boldsymbol{Q}_k$ and $\boldsymbol{R}_k$ are all diagonal matrices with equivalent elements. Therefore, the variance of the residual Δ_k is a diagonal matrix with equivalent elements ε_k. Applying Eqs. (44)-(46) and letting the hypothesis testing statistics be the constant threshold, the fault detectable in meters can be estimated as

$$r_k = \sqrt{\gamma_k^{\mathrm{T}} \gamma_k} = \sqrt{\varepsilon_k \chi^2_{m,\alpha}} \tag{47}$$

where ε_k is the sum of the equivalent diagonal elements of $\boldsymbol{Q}_k$ and $\boldsymbol{R}_k$.

C. MASTER FILTER AND FAULT DIAGNOSIS

This module consists of fault diagnosis and master filter, separately responsible for diagnosing, isolating fault and integrating state estimations of GPS sub-filter and COPS sub-filter. The fault is mainly identified according to Eq. (45).

In practical applications, the probability that both GPS and COPS become unreliable at the same time is very low. Hence, it is reasonable to assume that at least one sub-filter is reliable. These two sub-filters have different estimation error variance matrices, which can be used as a weighting coefficient for combining state estimates from above two sub-filters. Because the estimated states by master filter will be fed back, the fault-tolerant capability of the master filter is required to be relatively high so that the predicted position accuracy of kinematic model would not be severely deteriorated. Here, the fault state λ_k is viewed as reliability measure of corresponding state estimation, which can also be introduced as the weight of state estimation. Then, the combination of the above two state estimates can be written as:

$$\hat{\boldsymbol{\chi}} = (\lambda_G^{-1} \boldsymbol{P}_G^{-1} + \lambda_C^{-1} \boldsymbol{P}_C^{-1})^{-1} (\lambda_G^{-1} \boldsymbol{P}_G^{-1} \hat{\boldsymbol{\chi}}_G + \lambda_C^{-1} \boldsymbol{P}_C^{-1} \hat{\boldsymbol{\chi}}_C) \tag{48}$$

where $\boldsymbol{P}_G, \boldsymbol{P}_C$ are estimation error variance matrix of GPS and COPS, respectively. λ_G, λ_C are the Chi-squared test statistics of GPS and COPS, respectively. This combination

considers not only the accuracy indicated by $\boldsymbol{P}_G$ and $\boldsymbol{P}_C$, but also the reliability represented by λ_G and λ_C, which can be used to aid diagnosis. Note that before combining the state estimations, the test statistics is diagnosed. Once a fault is identified to be true, the corresponding state estimation is isolated, and the other state estimation will be adopted as the position of faulty UAV.

The procedure of this module can be depicted as follows:

1) Check fault state according to fault diagnosis rule.

2) If one sub-filter is diagnosed to be faulty, the state estimation of this sub-filter is isolated, and the other sub-filter is adopted.

3) If no fault is identified, the master filter will integrate two state estimates according to Eq. (46).

4) The integrated state estimation is fed back to kinematic model for prediction.

V. SIMULATIONS AND DISCUSSIONS

To simulate the cooperative flight of multiple UAVs, the dynamic model of UAV is adopted according to [14]. It is assumed that five UAVs are flying in the horizontal plane. One UAV's GPS becomes unreliable during the cooperative flight. Through RDF, whose measurement precision is 0.1 degrees, the faulty UAV tries to position itself through cooperative positioning system. The way points of five UAVs are listed in Table 1. Figure 4 depicts the authentic flight trajectory of five UAVs. In simulations, it is assumed that GPS fault occurs in the UAV5, and the other four UAVs are all reference UAVs to assist cooperative positioning. Once the GPS fault is confirmed, the corresponding UAV will never act as reference UAV.

TABLE 1. Flight way points of five UAVs.

No.	Coordinate (km)
UAV #1	(1 0), (5 0), (6 2), (5 4), (1 4), (0 2)
UAV #2	(20 1), (20 5), (18 6), (16 5), (16 1), (18 0)
UAV #3	(19 20), (15 20), (14 18), (15 16), (19 16), (20 18)
UAV #4	(0 19), (0 15), (2 14), (4 15), (4 19), (2 20)
UAV #5	(8 8), (12 8), (13 10), (12 12), (8 12), (7 10)

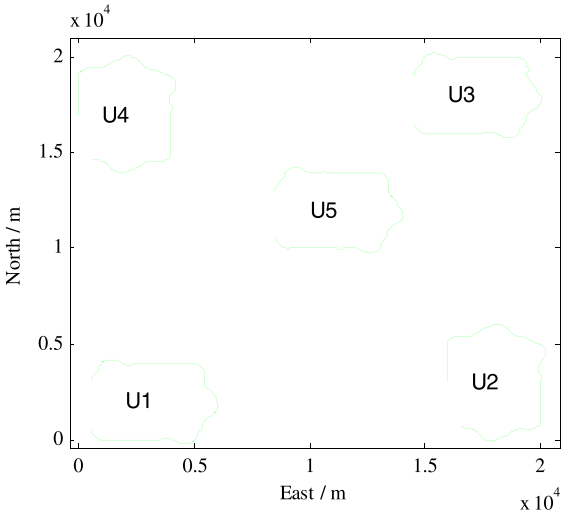

FIGURE 4. Flight trajectories of five UAVs under cooperative flight.

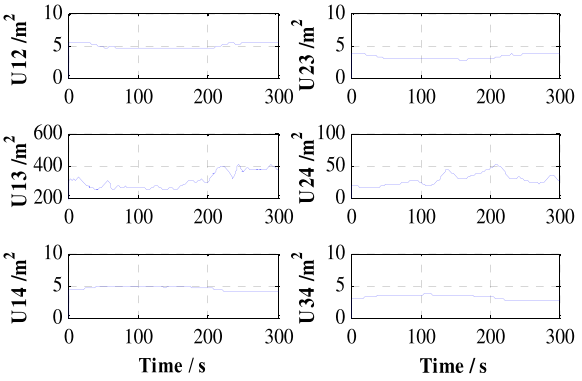

FIGURE 5. The HDOP values of six reference UAV sets ($\boldsymbol{U}_{ij}$ means reference set of $\boldsymbol{U}_i$ and $\boldsymbol{U}_j$).

A. COOPERATIVE POSITIONING UNDER COPS CASE

According to the flight trajectories given in Fig. 4, the UAV #5 tries to accomplish navigation only by using COPS. Since there are totally four reference UAVs, six sets of possible reference UAVs can be obtained. Applying the minimum HDOP principle, the optimal solution of the faulty UAV's position can be obtained. By comparing various HDOP values shown in Fig. 5, it is evident that the HDOP values of U12, U14, U23, and U34 are very close to each other. It is about 5 m^2. This is far smaller than U13 that varies from 250 to 400 m^2. Comparing the included azimuth angles of above five reference sets as shown in Fig. 6, the included azimuth angles of the previous four UAV sets are close to 90 or 270/-90 degrees, while U13 close to 180 degrees. In addition, both the HDOP value and the included azimuth angle of U24 are between the previous four reference sets (U12, U14, U23 and U34) and U13. It can be concluded that when the difference of two azimuth angles of one reference set is closer to $k\pi$, the HDOP value tends to be larger.

For various reference sets, statistics of observation error are listed in Table 2. The worst statistics belongs to the

TABLE 2. Statistics of positioning radial error.

U_1^r	U_2^r	Mean (m)	Variance (m^2)
1	2	26.41	205.38
1	3	186.25	17529
1	4	26.06	198.1
2	3	20.4	117.66
2	4	58.25	1719.1
3	4	20.55	147.27
The minimum HDOP		19.24	124.2

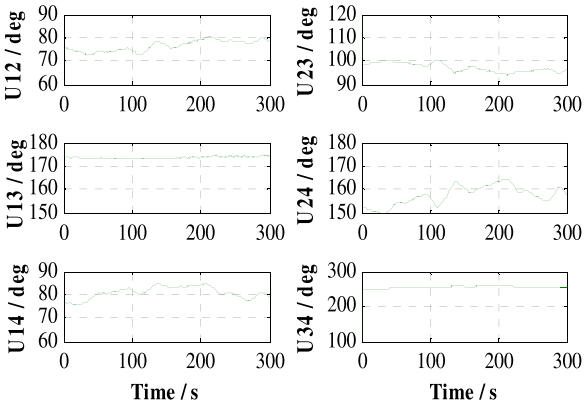

FIGURE 6. Included azimuth angles (difference of two relative azimuth angles) of six reference sets.

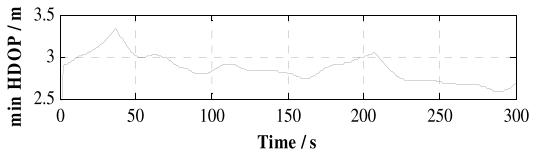

FIGURE 7. The minimum HDOP corresponding to optimal reference UAV set.

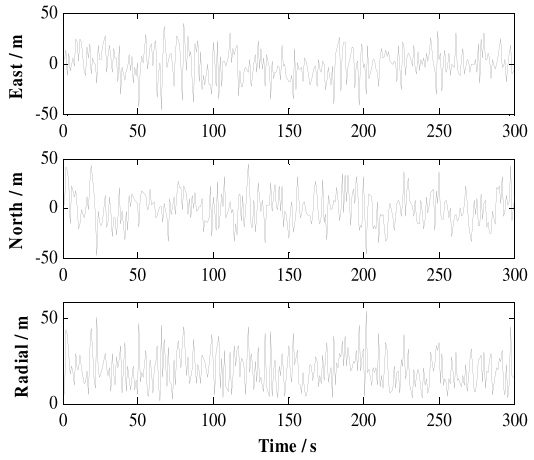

FIGURE 8. The observation error in various directions corresponding to the reference set with minimum HDOP.

U13 whose HDOP value is largest, which seems to be unreliable. U23 and U34 have the smallest mean of radial error, and their HDOP values tend to be smallest. U12 and U14 possess better statistics than U24. It is consistent with the HDOP value. One additional conclusion can be obtained is that the positioning error tends to be smaller as the HDOP value of one reference UAV set is smaller.

Figure 7 records the minimum HDOP selected from six various HDOP values as shown in Fig. 5. Based on this, the optimal positioning information can be obtained. The detailed observation and estimation errors are shown in Fig. 8. It demonstrates the observation error of COPS is not precise enough, since the absolute errors in the east and the north directions maximize almost to 50 m, and for radial

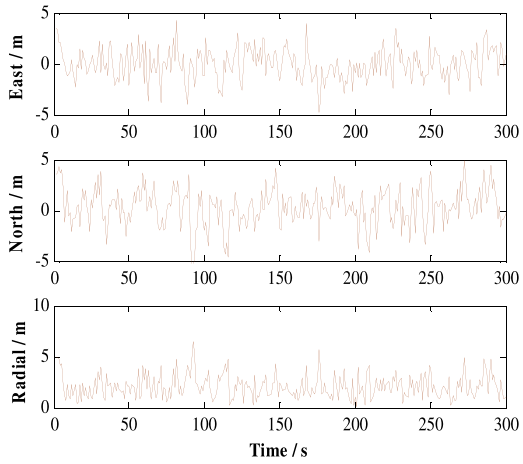

FIGURE 9. The estimation error from EKF in various directions corresponding to the reference set with minimum HDOP.

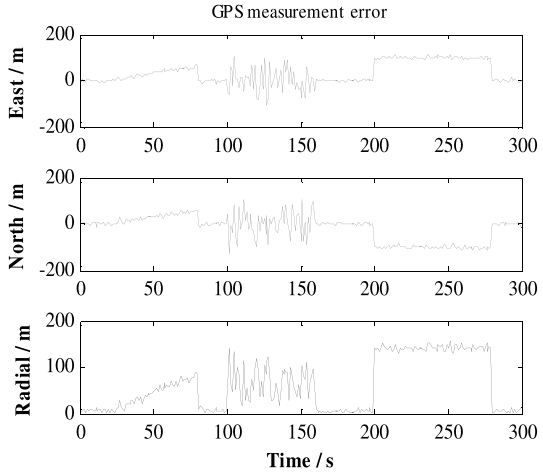

FIGURE 10. Three kinds of measurement error which are introduced to GPS.

error, the mean value is calculated to be 19.24 m as shown in Table 2. Although the optimal observation position is selected based on minimum HDOP value, it can still be optimized by applying extended Kalman filter. The superior estimation error is achieved as shown in Fig. 9. The eastern and the northern errors are both restrained within (-5, 5) m. The mean value in radial direction has been reduced to 2.13 m. It is about one-tenth of the original observation error.

B. FAULT-TOLERANT COOPERATIVE FLIGHT UNDER GPS FAULT CASE

1) CASE #1: ONLY ONE UAV LOST GPS SIGNAL

In this case, all the five UAVs are flying in a normal mode at the beginning. A GPS fault occurs to UAV5 at later. The COPS is assumed to be reliable. About 300 seconds flight is simulated. This period is seprated in three time intervals: (21, 80) seconds, (101, 160) seconds, and (201, 280) seconds, respectively. Three kinds of GPS faults are introduced.

Figure 10 shows three kinds of GPS faults: from the time 21 seconds to 80 seconds, the measurement error increases

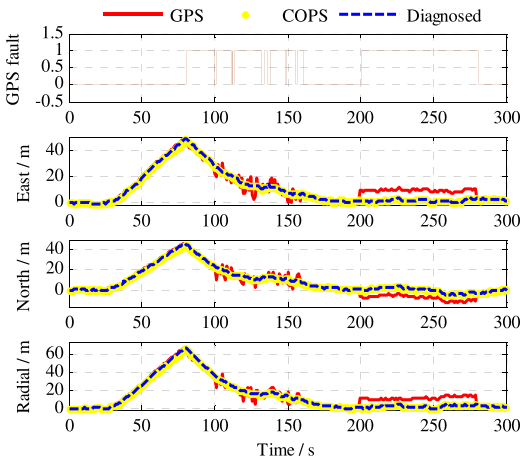

FIGURE 11. Diagnosis results of GPS fault and errors of GPS position estimation, COPS position estimation and diagnosed position estimation according to diagnosis results through threshold comparison without master filter integrating COPS and GPS.

gradually which may not be identified by fault diagnosis scheme. From the time 101 seconds to 160 seconds, this kind of error presents random noise with large amplitude and large variance, and the diagnosis result may vibrate as 'true' or 'false'. From time 201 seconds to 280 seconds, the error is introduced with significant drift, and it can be precisely identified to be faulty. To check the sensibility of fault diagnosis scheme to GPS measurement error, the threshold value for fault diagnosis rule is set as 41.45, which is determined according to the Chi-square table to guarantee confidence level high enough. The probability of false alarm α is no larger than 10^{-9} and the variance of GPS measurements in east or north direction is set as 25 m^2. Then, the minimum threshold of radial error is estimated about 32.5 m according to Eq. (47).

The diagnosis results of GPS fault as shown in Fig. 11 indicate that gradually increasing GPS position error from 21 seconds to 80 seconds cannot be identified as faulty. On the contrary, the healthy GPS positioning from 81 seconds to 100 seconds is diagnosed as faulty. Through observing the estimation error, it is easy to explain that since the error of integrated state estimation increases along with GPS error and then the integrated state estimation fed back to the kinematic model leads the prediction error to be increased. Therefore, the residual seems 'normal' as GPS error and prediction error grow at the same time. Then, when GPS returns to be healthy, the residual between the deviated predicted position of the kinematic model and the position of healthy GPS is large, and as a result, healthy GPS is mistakenly identified as faulty. The subsequent error after 100^{th} second decreases to be normal, since the GPS fault is precisely detected and the state estimation of COPS is selected as navigation information according to diagnosis results.

The fault diagnosis through threshold comparison is effective to handle the fault with abrupt abnormal positioning error. However, if the position error increases gradually, the fault may not be recognized immediately, and the feedback of state estimation will affect the predicted position of the kinematic model. As a result, the predicted position varies along with the gradually increasing position error. The simulation results are shown in Fig. 11. The purpose of generating such a large e fault scenario which covers abrupt and gradually increasing types of faults is to test capability and limitation of the developed fault diagnosis scheme for GPS faults handling.

In this paper, the master filter introduced in Section IV.C is designed for the problem of wrong fault diagnosis as shown in Fig. 11. The diagnosis results of GPS fault are shown in Fig. 12. The increasing error can be finally identified after a time delay of about 27 seconds. From time 81 seconds to 100 seconds, the problem of identifying healthy GPS as faulty is resolved. Even though the increasing error cannot be detected immediately, the error of integrated state estimation is reduced through combining state estimations of COPS and GPS. As GPS error increaseing, the reliability of GPS will decrease. The weight of GPS becomes lower according to Eq. (46) and the weight of COPS becomes relatively higher. Then, the error of integrated state estimation becomes smaller than GPS error. The difference will be larger and larger as GPS error keeps increasing gradually. Once the difference is large enough, the residual of GPS position can be detected and diagnosed as faulty, and the state estimation of GPS will be isolated. Once GPS fault is detected, the position provided by COPS will be selected as integrated state estimation through employing an extended Kalman filter. Overall, the integrated estimation errors are well restrained within -5 m to 5 m in East and North directions, and 0 to 5 m in the radial direction as shown in Fig. 12. This is reliable enough for navigation.

2) CASE #2: TWO UAVS LOST GPS SIGNAL

In the preceding case, the simulated experiment indicates that the continuous increasing error in GPS could be diagnosed but with a time delay of about 27 seconds. During this time

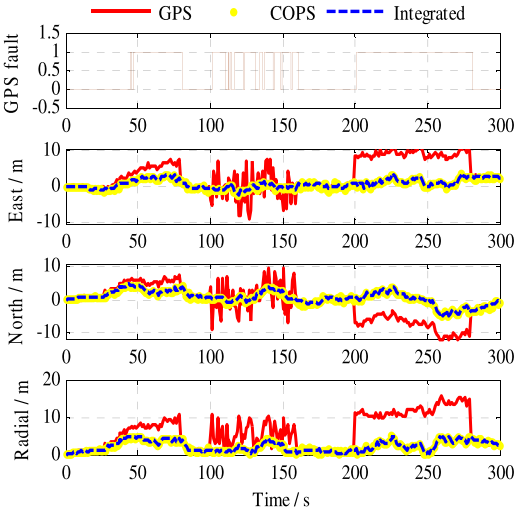

FIGURE 12. Diagnosis results of GPS fault and errors of GPS position estimation, COPS position estimation and integrated position estimation of COPS and GPS according to diagnosis results and master filter.

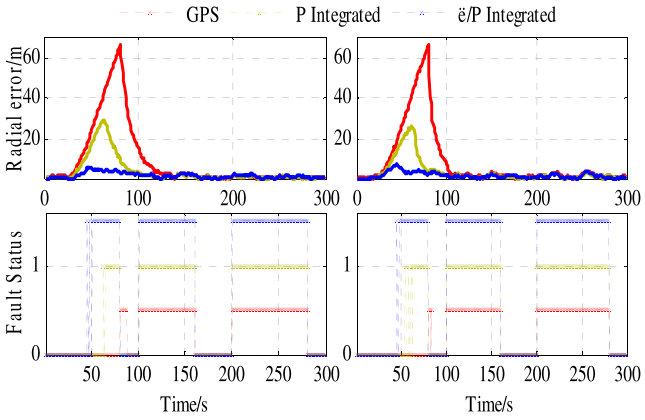

FIGURE 13. Diagnosis results of GPS fault and radial position errors of GPS, GPS/COPS integrated with only variance P as weight, and GPS/COPS integrated with hypothesis testing statistics λ and variance P_k as weights. The left two figures record the information of UAV 3, and right two records UAV 4. Besides, the fault status 'low' is indicated by 0 and 'high' indicated by 0.5, 1 and 1.5 identically.

delay, the undiagnosed ''healthy'' UAV might be adopted as referenced by any other UAV. Hence, such a situation is assumed as two UAVs, U3 and U4, suffered identical GPS abnormity at the same time. The GPS error is modeled as the same as in Fig. 10, but errors from 100 seconds to 150 seconds are replaced as drift error. Three methods are applied to the UAVs' positioning respectively: M#1) KF for GPS, M#2) integrated KF for GPS/COPS with estimation variance weighted, and M#3) combined KF for GPS/COPS with hypothesis testing statistics λ and estimation variance $\boldsymbol{P_k}$ weighted as proposed in this paper.

The fault status results illustrated in Fig. 13 show that the method M#3 proposed by this paper diagnosed the increasing GPS error earlier than method M#2 despite a time delay, and method M#1 cannot diagnose GPS as faulty from 20 seconds to 80 seconds but as 'faulty' at time 81 seconds falsely. The rest drift error can be diagnosed by three methods. On the other hand, the radial error is evidently reduced by applying the proposed method M#3 compared to method M#2. Since the estimation variance describes the long-term statistical feature of state estimation but the test statistics focuses on current quality, the proposed method M#3 can reduce the abnormal error immediately. The reduced errors contained in position estimation guarantee well the predicted position error smaller than GPS error, and the COPS in other UAVs would not be severely influenced when referring to the faulty UAV. Thus, though two UAVs suffered GPS errors at the same time, the proposed method in this paper can also guarantee the accuracy of position estimation and successfully diagnose faulty GPS.

VI. CONCLUSIONS

Using the relative angle information among UAVs, the multiple UAVs cooperative positioning has been achieved in the presence of GPS fault occurring to one of the multiple UAVs during cooperative/formation flight. Using the minimum horizontal dilution of positioning principle, the positioning accuracy is well guaranteed through finding out optimal position with relatively smallest observation error. Extended Kalman filter is employed to optimize the observation position of the faulty UAV and good accuracy has been achieved. By simulating cooperative flight of multiple UAVs in the presence of GPS fault, the proposed COPS/GPS fault-tolerant navigation algorithm is proved to be effective. Although the results are obtained in horizontal plane, this method can be easily extended to the three-dimensional space. As one of future works, based on the fault tolerant positioning approach proposed in the paper, fault tolerant controller design for multiple UAVs formation flying with system uncertainty, external disturbance, and input saturation, should be carried by referring to the results in [25]– [30].

REFERENCES

[1] M. Bryson and S. Sukkarieh, ''Co-operative localisation and mapping for multiple UAVs in unknown environments,'' in *Proc. IEEE/RSJ Int. Conf. Intell. Robots Syst.*, Mar. 2007, pp. 1–12.

[2] W. Kang and H.-H. Yeh, ''Co-ordinated attitude control of multi-satellite systems,'' *Int. J. Robust Nonlinear Control*, vol. 12, nos. 2–3, pp. 185–205, 2002.

[3] J. M. Fowler and R. D'Andrea, ''Distributed control of close formation flight,'' in *Proc. IEEE 41st Conf. Decision Control*, Dec. 2002, pp. 2972–2977.

[4] A. Proud and M. Pachter, ''Close formation flight control,'' in *Proc. AIAA Guid. Navigat. Control Conf. Exhib.*, 1999, pp. 1231–1246.

[5] R. W. Beard, T. W. McLain, M. A. Goodrich, and E. P. Anderson, ''Coordinated target assignment and intercept for unmanned air vehicles,'' *IEEE Trans. Robot. Autom.*, vol. 18, no. 6, pp. 911–922, Dec. 2002.

[6] J. S. Bellingham, M. Tillerson, J. P. How, and M. Alighanbari, ''Cooperative path planning for multiple UAVs in dynamic and uncertain environments,'' in *Proc. IEEE 41st Conf. Decision Control*, Dec. 2002, pp. 2816–2822.

[7] M. Golestani, I. Mohammadzaman, M. J. Yazdanpanah, and A. R. Vali, ''Application of finite-time integral sliding mode to guidance law design,'' *ASME J. Dyn. Syst., Meas., Control*, vol. 137, no. 11, pp. 114501-1–114501-4, 2015.

[8] M. Golestani and I. Mohammadzaman, ''PID guidance law design using short time stability approach,'' *Aerosp. Sci. Technol.*, vol. 43, pp. 71–76, Jun. 2015.

[9] M. Golestani, I. Mohammadzaman, and A. R. Vali, ''Finite-time convergent guidance law based on integral backstepping control,'' *Aerosp. Sci. Technol.*, vol. 39, pp. 370–376, Dec. 2014.

[10] Y. Zhang and J. Jiang, ''Bibliographical review on reconfigurable fault-tolerant control systems,'' *Annu. Rev. Control*, vol. 32, no. 2, pp. 229–252, 2008.

[11] X. Yu and J. Jiang, ''Hybrid fault-tolerant flight control system design against partial actuator failures,'' *IEEE Trans. Control Syst. Technol.*, vol. 20, no. 4, pp. 871–886, Jul. 2012.

[12] X. Yu, Z. Liu, and Y. Zhang, ''Fault-tolerant flight control design with finite-time adaptation under actuator stuck failures,'' *IEEE Trans. Control Syst. Technol.*, vol. 25, no. 4, pp. 1431–1440, Jul. 2016.

[13] X. Yu, Y. Zhang, and Z. Liu, ''Fault-tolerant flight control design with explicit consideration of reconfiguration transients,'' *J. Guid., Control, Dyn.*, vol. 39, no. 3, pp. 556–563, 2015.

[14] C.-C. Chen, S. S.-D. Xu, and Y.-W. Liang, ''Study of nonlinear integral sliding mode fault-tolerant control,'' *IEEE/ASME Trans. Mechatronics*, vol. 21, no. 2, pp. 1160–1168, Apr. 2016.

[15] R. Sven, ''Developement of a INS/GPS navigation loop for an UAV,'' M.S. thesis, Luleå Univ. Technol., Luleå, Sweden, 2000.

[16] W. Ding *et al.*, ''Adding optical flow into the GPS/INS integration for UAV navigation,'' in *Proc. Int. Global Navigat. Satellite Syst. Soc. IGNSS Symp.*, 2009, pp. 1–13.

[17] J. Chen, D. M. Dawson, M. Selah, and T. Burg, ''Multiple UAV navigation with finite sensing zone,'' in *Proc. Amer. Control Conf.*, Jun. 2006, p. 6.

[18] Y. H. Qu and Y. Zhang, "Cooperative localization against GPS signal loss in multiple UAVs flight," *J. Syst. Eng. Electron.*, vol. 22, no. 1, pp. 103–112, Feb. 2011.
[19] D. M. Stipanović, G. Inalhan, R. Teo, and C. J. Tomlin, "Decentralized overlapping control of a formation of unmanned aerial vehicles," in *Proc. IEEE 41st Conf. Decision Control*, Dec. 2002, pp. 2829–2835.
[20] F. Kendoul and K. Nonami, "A visual navigation system for autonomous flight of micro air vehicles," in *Proc. IEEE/RSJ Int. Conf. Intell. Robots Syst.*, Oct. 2009, pp. 3888–3893.
[21] S.-M. Oh and E. N. Johnson, "Relative motion estimation for vision-based formation flight using unscented Kalman filter," in *Proc. AIAA Guid. Navigat. Control Conf. Exhib.*, 2007, pp. 20–23.
[22] M. S. Batson and J. C. McEachen, "A method for fast radio frequency direction finding using wireless sensor networks," in *Proc. 41st Annu. Int. Conf. Syst. Hawaii Int. Conf. Syst. Sci.*, Jan. 2008, pp. 1530–1605.
[23] D. Caratelli, I. Liberal, and L. Yarovoy, "Design and full-ware analysis of conformal ultra-wideband radio direction findings," *IET Microw. Antennas Propag.*, vol. 5, no. 10, pp. 1164–1174, Jul. 2011.
[24] F. Nivole, C. Brousseau, S. Avrillon, D. Lemur, and L. Bertel, "Radio direction finding applied to DVB-T network for vehicular mobile reception," in *Proc. 3rd Eur. Conf. Antennas Propag.*, Mar. 2009, pp. 3297–3301.
[25] X. Yu, Y. Fu, and Y. Zhang, "Aircraft fault accommodation with consideration of actuator control authority and gyro availability," *IEEE Trans. Control Syst. Technol.*, to be published, doi: 10.1109/TCST.2017.2707378.
[26] B. Xiao and S. Yin, "Velocity-free fault-tolerant and uncertainty attenuation control for a class of nonlinear systems," *IEEE Trans. Ind. Electron.*, vol. 63, no. 7, pp. 4400–4411, Jul. 2016.
[27] B. Xiao, S. Yin, and O. Kaynak, "Tracking control of robotic manipulators with uncertain kinematics and dynamics," *IEEE Trans. Ind. Electron.*, vol. 63, no. 10, pp. 6439–6449, Oct. 2016.
[28] B. Xiao, S. Yin, and L. Wu, "A structure simple controller for satellite attitude tracking maneuver," *IEEE Trans. Ind. Electron.*, vol. 64, no. 2, pp. 1436–1446, Feb. 2017.
[29] X. Zhao, P. Shi, X. Zheng, and J. Zhang, "Intelligent tracking control for a class of uncertain high-order nonlinear systems," *IEEE Trans. Neural Netw. Learn. Syst.*, vol. 27, no. 9, pp. 1976–1982, Sep. 2015.
[30] X. Zhao, H. Yang, W. Xia, and X. Wang, "Adaptive fuzzy hierarchical sliding mode control for a class of MIMO nonlinear time-delay systems with input saturation," *IEEE Trans. Fuzzy Syst.*, to be published, doi: 10.1109/FTUZZ.2016.2594273.

YAOHONG QU received the M.S. and Ph.D. degrees in control theory and control engineering from Northwestern Polytechnical University, China, in 2002 and 2006, respectively. He was an Assistant Engineer with the Xi'an Navigation Technology Institute from 1996 to 1999, and then he became a Lecturer and an Associate Professor with the School of Automation, Northwestern Polytechnical University, in 2006 and 2011, respectively. He was a Visiting Scientist with the Department of Mechanical and Industrial Engineering, Concordia University, Canada, from 2009 to 2010. His research interests are navigation and flight control of UAV, multi-UAV cooperative control, and wind field estimation in flight. He is currently an Unmanned System Program Committee Member of AIAA.

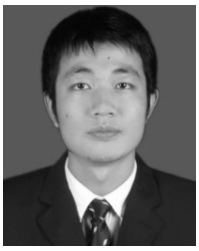

JIZHI WU received the M.S. degree in control theory and control engineering from the School of Automation, Northwestern Polytechnical University, Xi'an China, in 2012. He is currently with the Department of Flight Control System, Commercial Aircraft Corporation of China Ltd., Shanghai, China. His research interests include the flight control law design, multi-Body dynamics/kinematics, and redundancy architecture of flight control system.

BING XIAO received the B.S. degree in mathematics from Tianjin Polytechnic University, Tianjin, China, in 2007, and the M.S. and Ph.D. degrees in engineering from the Department of Control Science and Engineering, Harbin Institute of Technology, Harbin, China, in 2010 and 2014, respectively.

He is currently a Professor with the College of Engineering, Bohai University, Jinzhou, China. His current research interests include spacecraft attitude control, fault diagnosis, fault-tolerant control, robot control, and mechatronics.

DONGLI YUAN received the M.S. degree and the Ph.D. degree in control theory and engineering from Northwestern Polytechnical University, China, in 1999 and 2004, respectively. She was a Visiting Scholar with the Aviation Engineering Department, Cranfield University, U.K., in 2014. She is currently an Associate Professor with Northwestern Polytechnical University. She has authored over 30 peer-reviewed papers in journals and conference proceedings. Her research interests are in application of control theory, flight control, and navigation control.